MODELING TRAVEL-TIME CORRELATIONS BASED ON SENSITIVITY KERNELS AND CORRELATED VELOCITY ANOMALIES

William L. Rodi[1] and Stephen C. Myers[2]

Massachusetts Institute of Technology[1] and Lawrence Livermore National Laboratory[2]

Sponsored by National Nuclear Security Administration

Contract No. DE-FC52-05NA26603[1] and DE-AC52-07NA27344[2]

Proposal No. BAA05-14

ABSTRACT

This project concerns the errors in predicted regional and teleseismic travel times resulting from velocity heterogeneity in the real Earth not represented in the reference Earth model used for travel-time calculation. We are developing techniques for calculating the covariances between such prediction errors associated with different event-station paths, based on a statistical characterization of the velocity heterogeneity and the theoretical travel-time sensitivity to the Earth's velocity structure for each path. This effort is motivated by previous discoveries that event location errors can be reduced when a locator uses the full covariance matrix for travel-time prediction errors, including off-diagonal elements to account for correlations. Moreover, a physical model for travel-time covariances potentially provides useful constraints in the construction of empirical travel-time correction surfaces. We have developed numerical algorithms that generate a covariance matrix for first-arrival P-wave travel times along paths to various station locations from a fixed event location. Calculations with various station geometries reveal a strong dependence of the travel-time variances and covariances on the spatial sampling of seismic rays. For example, we find that prediction-error variances are smaller for teleseismic P arrivals than for Pn arrivals since teleseismic rays travel a shorter, more vertical path in the upper mantle, whereas most of the Pn path is in the upper mantle where velocity heterogeneity is greatest. Our calculated travel-time variance vs. distance curve agrees well with empirical results for a Eurasian data set when the standard deviation of velocity heterogeneity decreases from 2% to 1% at the 410 km discontinuity. We further find that correlation between travel times can be parameterized by inter-station distance only when both stations observe the same travel-time branch, but distinct breaks in residual correlation occur at the cross-over of branches. Thus, our calculations show small travel-time correlation between a teleseismic P arrival and a Pn arrival at different stations, even when the stations are close to one another. Last, we are currently investigating the effects of finite frequency sensitivity kernels on travel-time correlation. In the preliminary work presented here, we estimate the spatial extent of finite-frequency kernels by computing delay times for paths off of the geometrical ray. We find that the sensitivity of 1-Hz Pn arrivals are sensitive to the entire velocity profile between the Moho and a maximum depth that reaches 200 km for an arrival at 15° distance, suggesting that prediction errors in regional and far-regional travel times will be correlated over distance separations well exceeding the correlation length of velocity heterogeneity.

Report Documentation Page

Form Approved
OMB No. 0704-0188

Public reporting burden for the collection of information is estimated to average 1 hour per response, including the time for reviewing instructions, searching existing data sources, gathering and maintaining the data needed, and completing and reviewing the collection of information. Send comments regarding this burden estimate or any other aspect of this collection of information, including suggestions for reducing this burden, to Washington Headquarters Services, Directorate for Information Operations and Reports, 1215 Jefferson Davis Highway, Suite 1204, Arlington VA 22202-4302. Respondents should be aware that notwithstanding any other provision of law, no person shall be subject to a penalty for failing to comply with a collection of information if it does not display a currently valid OMB control number.

1. REPORT DATE	2. REPORT TYPE	3. DATES COVERED
SEP 2008		**00-00-2008 to 00-00-2008**

4. TITLE AND SUBTITLE	5a. CONTRACT NUMBER
Modeling Travel-Time Correlations Based on Sensitivity Kernels and Correlated Velocity Anomalies	5b. GRANT NUMBER
	5c. PROGRAM ELEMENT NUMBER
6. AUTHOR(S)	5d. PROJECT NUMBER
	5e. TASK NUMBER
	5f. WORK UNIT NUMBER
7. PERFORMING ORGANIZATION NAME(S) AND ADDRESS(ES) **Lawrence Livermore National Laboratory,PO Box 808,Livermore,CA,94551-0808**	8. PERFORMING ORGANIZATION REPORT NUMBER
9. SPONSORING/MONITORING AGENCY NAME(S) AND ADDRESS(ES)	10. SPONSOR/MONITOR'S ACRONYM(S)
	11. SPONSOR/MONITOR'S REPORT NUMBER(S)

12. DISTRIBUTION/AVAILABILITY STATEMENT
Approved for public release; distribution unlimited

13. SUPPLEMENTARY NOTES
Proceedings of the 30th Monitoring Research Review: Ground-Based Nuclear Explosion Monitoring Technologies, 23-25 Sep 2008, Portsmouth, VA sponsored by the National Nuclear Security Administration (NNSA) and the Air Force Research Laboratory (AFRL)

14. ABSTRACT
see report

15. SUBJECT TERMS

16. SECURITY CLASSIFICATION OF:			17. LIMITATION OF ABSTRACT	18. NUMBER OF PAGES	19a. NAME OF RESPONSIBLE PERSON
a. REPORT	b. ABSTRACT	c. THIS PAGE			
unclassified	**unclassified**	**unclassified**	**Same as Report (SAR)**	**10**	

OBJECTIVE

To achieve accurate event locations and estimates of location uncertainty, seismic event location algorithms must account for two types of errors: *pick* errors in the measured arrival times of the seismic phases observed at various stations, and *model* errors incurred in predicting the travel times of observed station/phase combinations as a function of the event location. Model errors are attributable to velocity anomalies in the Earth that are not rendered in the velocity model used for travel-time prediction. When the observing stations are sufficiently close to one another, their model errors are expected to be correlated. While it is now standard practice for event location algorithms used in nuclear monitoring to assign error *variances* that include the contribution from model prediction errors, the algorithms generally set the error *covariances* to zero; correlations are ignored. Doing so can seriously degrade location accuracy when the distribution of seismic stations is far from uniform (Chang et al., 1983; Yang et al., 2004).

This project is investigating the phenomenon of correlated travel-time prediction errors from a physical point of view, making use of the principles of wave propagation through heterogeneous media and our knowledge of the statistical properties of the Earth's heterogeneity. Specifically, we are developing techniques to calculate covariance matrices of travel-time model errors by integrating travel-time sensitivity kernels with plausible correlation functions describing the Earth's velocity heterogeneity. This paper summarizes our approach and reports some numerical calculations designed to determine how travel-time prediction variances and correlations depend on the epicentral distance from an event. We also report a preliminary investigation into the importance of finite-frequency effects of travel-time covariances.

RESEARCH ACCOMPLISHED

Approach

Given a set of n arrival time data from an event, one can decompose the data errors as (for $i = 1,\ldots,n$)

$$e_i = e_{\mathrm{p},i} + e_{\mathrm{m},i}, \tag{1}$$

where the first term is the *pick*, or measurement, error and the second term is the *model* error, or error in the travel time predicted by a reference velocity model. Typically, event location algorithms assume that the errors of both types have a zero mean and a diagonal $n \times n$ variance/covariance matrix, leading to a diagonal covariance matrix for the total errors. The errors for different i are thus assumed to be uncorrelated. We are addressing the problem of calculating a full covariance matrix for model errors, having components $\sigma_{\mathrm{m},ij}$ defined by

$$\sigma_{\mathrm{m},ij} = \mathrm{E}[e_{\mathrm{m},i}\, e_{\mathrm{m},j}]. \tag{2}$$

E[ ] denotes the expectation operator.

To explain our approach to covariance modeling, we consider only P-wave arrivals. Let $v_0(\mathbf{x})$ denote the P velocity function for the reference model, and $v_E(\mathbf{x})$ denote the Earth's true (and unknown) velocity function. Then, model errors can be linked to the slowness difference, which we denote $m(\mathbf{x})$:

$$m(\mathbf{x}) = v_E^{-1}(\mathbf{x}) - v_0^{-1}(\mathbf{x}). \tag{3}$$

We assume that the travel-time dependence on slowness can be adequately approximated as linear, allowing us to express the model error in the ith datum as

$$e_{\mathrm{m},i} = \int d\mathbf{x}\; a_i(\mathbf{x})\, m(\mathbf{x}), \tag{4}$$

where $a_i(\mathbf{x})$ is the first-order sensitivity kernel of the ith travel-time prediction function, as evaluated at v_0. In the high-frequency limit, this kernel is concentrated along the geometrical ray connecting the event and station locations. For finite frequency, it is spatially distributed around this ray. In either case, we point out that the model error is a function of the event *and* station locations.

We consider $m(\mathbf{x})$ to be a Gaussian random field having zero mean and a specified covariance between any two points, described by a covariance operator $C(\mathbf{x}, \mathbf{x}')$:

$$\mathrm{E}[m(\mathbf{x})] = 0 \tag{5}$$

$$\mathrm{E}[m(\mathbf{x})\, m(\mathbf{x}')] = C(\mathbf{x}, \mathbf{x}'). \tag{6}$$

The covariance between two model errors is then given by

$$\sigma_{\mathrm{m},ij} = \int d\mathbf{x}\; a_i(\mathbf{x}) \int d\mathbf{x}'\; C(\mathbf{x}, \mathbf{x}')\, a_j(\mathbf{x}'). \tag{7}$$

Equation (7) implies that the extent to which two model errors are correlated depends on the spatial relationship between their sensitivity kernels in relation to the correlation structure of the velocity field.

Covariance Modeling Algorithms

A flexible and numerically advantageous approach to characterizing nonstationary random fields is to specify the covariance operator indirectly through its operator inverse, which we denote D, such that

$$DC(\mathbf{x}, \mathbf{x}') = \delta(\mathbf{x} - \mathbf{x}'). \tag{8}$$

If we take D to be a differential operator, then $C(\mathbf{x}, \mathbf{x}')$ is its Green's function. Following Rodi et al. (2003), we have implemented this approach with D as (in spherical coordinates)

$$D = \frac{\mathrm{const}}{\lambda_1^2 \lambda_2 \sigma^2} \left[\delta(\mathbf{x}) - \frac{1}{(2\ell - 3)} \left(\frac{\lambda_1^2}{r^2} \nabla_1^2 + \lambda_2^2 \frac{\partial^2}{\partial r^2} \right) \right]^{\ell}, \quad \ell \geq 2. \tag{9}$$

Here ∇_1^2 is the horizontal Laplacian operator; λ_1 and λ_2 are horizontal and vertical correlation lengths, respectively; and σ^2 is the variance of the slowness. The order of the operator, ℓ, controls how $C(\mathbf{x}, \mathbf{x}')$ decays as the distance between $\mathbf{x}$ and $\mathbf{x}'$ increases. We take $\ell = 2$, which leads to an exponential decay. In this approach, nonstationarity results from three effects: (1) a boundary condition at the Earth's surface, (2) de-correlation of velocity anomalies across interfaces, such as the Moho, and (3) allowing spatial dependence of σ, λ_1 and λ_2.

In previous years we developed two numerical methods for evaluating the double integral of equation (7), given that the inverse velocity covariance operator D is specified. These algorithms are described in Rodi and Myers (2007).

Distance Dependence of Travel-Time Covariance

To investigate the dependence of travel-time covariances on epicentral distance, we applied our numerical modeling approach to a north-south linear array of 70 stations equally spaced from 0.5° to 35° in epicentral distance from a nominal event location at 0°N, 0°E. The resulting 70×70 covariance matrix then reveals the dependence of travel-time variance on distance and of travel-time correlation on distance and distance separation between stations. The calculations were done using travel-time sensitivities implied by

Table 1: Geostatistical parameters for numerical examples

	Case A	*Case B*
Velocity std. dev. (σ)		
Crust	3%	3%
Mantle ($z \leq 410$)	1.5%	2%
Mantle ($z > 410$)	1.5%	1%
Horiz. correlation length (λ_1)	300 km	300 km
Vertical correlation length (λ_2)		
Crust	17.5 km	17.5 km
Mantle	60 km	60 km

geometrical ray theory, ignoring finite-frequency effects. Geometrical rays were evaluated with the *ak135* 1D Earth model (Kennett et al., 1995) and transformed to discrete sensitivities for a 3D model parameterization.

We performed the calculations under two assumptions about the geostatistical parameters of velocity heterogeneity, as listed in Table 1. The correlation distances are the same for both cases: $\lambda_1 = 300$ km, $\lambda_2 = 17.5$ km in the crust and 60 km in the mantle. The standard deviation of velocity variations in the crust was also common to both cases: $\sigma = 3\%$. The two geostatistical models differ in the standard deviation assigned to the mantle velocity. The first model (Case A) used $\sigma = 1.5\%$ throughout the mantle. Case B had $\sigma = 2\%$ in the upper mantle (above the 410-km discontinuity) and $\sigma = 1\%$ below 410 km.

Figure 1 shows the resulting standard deviations of travel-time model errors, derived from the diagonal elements of the 70×70 covariance matrix and plotted versus epicentral distance. Discontinuities in the travel-time standard deviation are evident at the same distances in both cases of geostatistical parameters. These discontinuities are directly attributed to discontinuities in ray parameter, which are controlled by the *ak135* model. From approximately 2° to 15° travel-time error increases consistently, but not strictly linearly. The rate of increase in the error diminishes with distances, as rays begin to average over several correlation lengths of velocity variations. At approximately 15°, rays begin to dive deeper into the upper mantle and travel more vertically, resulting in more averaging over the shorter correlation-length anomalies in the vertical dimension. Several breaks in the error structure are evident as rays dive below the 410-km velocity discontinuity and then the 660-km discontinuity. Error structure stabilizes at teleseismic distances ($\geq 24°$) when rays bottom in the lower mantle and the ray parameter remains continuous. Travel-time error is lower at teleseismic distance because vertically traveling rays in the more strongly heterogeneous upper mantle average over more wavelengths of geologic heterogeneity, recalling that we assumed the vertical scale of heterogeneity to be much smaller than the horizontal scale.

The red line in each panel of Figure 1 is an empirical travel-time error vs. event-station distance relation we inferred from observations in the LLNL ground-truth database of events for Eurasia and Africa (Ruppert et al., 2005). First-arriving P-waves were used for events meeting the GT criteria of Bondar et al. (2004) or whose location was constrained by non-seismic means (e.g., known explosions, mine collapses, earthquakes with InSAR signals). We used a methodology similar to Flanagan et al. (2007) to assess travel-time prediction (model) error. We began by selecting only stations with sufficient data for distance-dependent variance estimation (at least 10 arrivals in each 1° event-station distance bin). For each station, we assessed pick (random) error by computing the standard deviation of residuals for clusters of events within 20 km of one another. The random error for many event clusters was used to determine pick error as a function of station-event distance. We subtracted distant-dependent pick error variance from travel-time residual variance to estimate distance-dependent model-error variance. The final curve, shown in each panel of Figure 1, was obtained as an average of the model-error curve for stations throughout

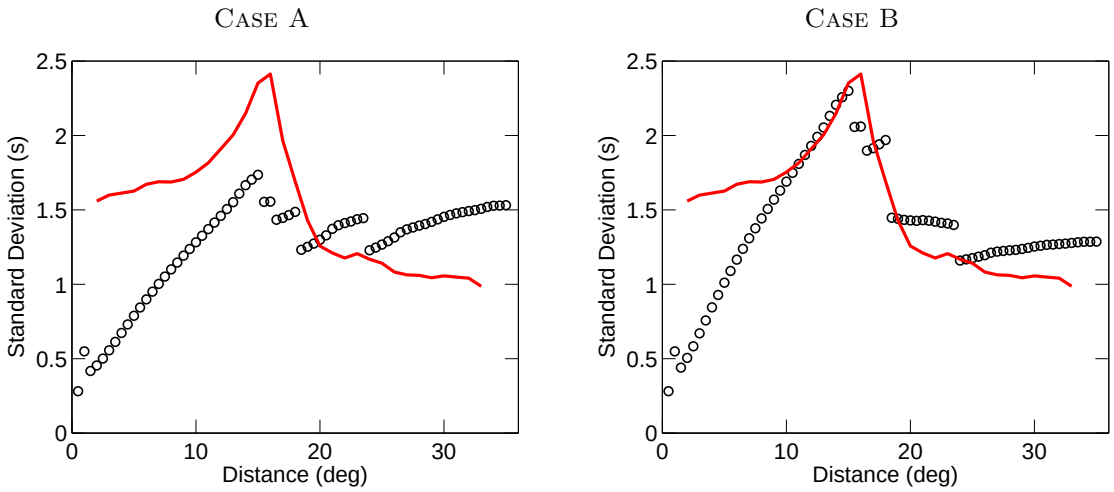

Figure 1: Model-based standard deviation of travel-time prediction error as a function of epicentral distance, plotted as black circles and derived with two different geostatistical models of velocity heterogeneity (Cases A and B of Table 1). The cases differ in their assumption about the magnitude of mantle heterogeneity (σ), with the left panel assuming $\sigma = 1.5\%$ everywhere in the mantle, and the right panel assuming $\sigma = 2\%$ in the upper mantle ($z \leq 410$ km) and $\sigma = 1\%$ below 410 km. In each panel, the red line displays an empirically derived standard-deviation vs. distance curve.

Eurasia and Africa. Comparing the left and right panels of the figure, it is clear that our Case B calculations of travel-time standard deviation are much more consistent with the empirically derived curve than are the Case A calculations, suggesting that a geostatistical model concentrating heterogeneity in the upper mantle is more realistic.

Figure 2 displays the model-based correlation matrix corresponding to the standard deviations shown in Figure 1. Only Case B is shown since the correlation matrices for the two cases were nearly identical. Analogous to the breaks in travel-time standard deviation, the correlation matrix, which is ordered by event-station distance, shows a roughly block-diagonal structure with the blocks delimited by the same cross-over distances and associated jumps in ray parameter. These results demonstrate that simple estimates of travel-time correlation based on the distance between stations do not adequately account for correlations between travel times near cross-over distances. If two stations straddle a break in ray parameter, then travel-time residuals are likely to be weakly correlated. This result has profound implications for both location algorithms and empirical methods (e.g., kriging) that make use of the travel-time residual covariance matrix.

Travel-Time Correlation vs. Latitude and Longitude

In this example, we computed the travel-time covariance matrix for each of six station arrays, varying in distance from a nominal event location at 0°N, 0°E. Each array contained 169 stations in a 13×13 square with 1° spacing in latitude and longitude. The computations were done with *ak135* sensitivities for infinite-frequency travel times.

The results are shown in Figure 3. Each panel corresponds to one of the six arrays and plots the travel-time correlation coefficient between the center station (marked with a white dot) and the other stations of the array. The results show clearly the nonstationarity of travel-time model errors as a function of station location, evident as discontinuities in correlation coefficient with distance, as were seen in

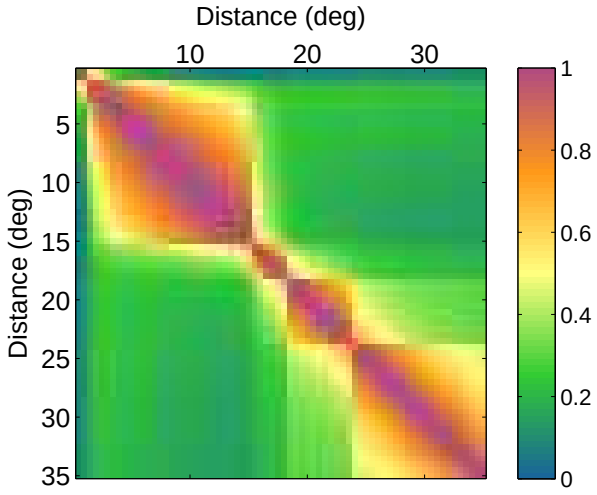

Figure 2: Correlation coefficient between prediction errors at different epicentral distances and a common azimuth, computed with the Case B geostatistical parameters listed in Table 1.

Figure 2. Figure 3 also allows us to see the azimuthal dependence of travel-time correlations. The azimuthal dependence, for each fixed distance, is not overtly nonstationary and appears to reflect the assumed horizontal correlation length of the velocity field (300 km).

Finite-Frequency Effects

Since arrival times are measured from seismograms having a finite bandwidth in frequency, their sensitivity to the Earth's velocity structure is distributed in a finite volume around the geometrical raypath. The theory of finite-frequency travel times has been developed by a number of authors (Marquering et al., 1999; Zhao et al., 2000; Dahlen et al., 2000; Hung et al., 2000). The resulting *banana-doughnut* sensitivity kernels have a spatial extent that can be related to the *delay-time* function given by

$$\tau(\mathbf{x}) = T(\mathbf{x}, \mathbf{x}_r) + T(\mathbf{x}, \mathbf{x}_s) - T(\mathbf{x}_r, \mathbf{x}_s), \tag{10}$$

where $\mathbf{x}_s$ denotes the source position and $\mathbf{x}_r$ the receiver position, and where the function $T(\mathbf{x}, \mathbf{x}')$ defines the (infinite-frequency) travel time between arbitrary points $\mathbf{x}$ and $\mathbf{x}'$. The maximum sensitivity of a banana-doughnut kernel for frequency ω occurs when

$$\tau(\mathbf{x}) = \frac{\pi}{2\omega}, \tag{11}$$

i.e. points at which the delay time is one-fourth the temporal period.

We have begun to consider whether finite-frequency effects would significantly alter our model-based travel-time covariances, even for the relatively high-frequency signals used in picking times for earthquake location. The effect would be potentially significant if the spatial extent of a travel-time sensitivity kernel were comparable to, or larger than, the correlation length of velocity heterogeneity. To quantify this, we have computed delay-time functions for regional and teleseismic paths, using *ak135* as the reference model for travel-time calculation.

Figure 4 shows maps of delay time versus geographic position for paths to four stations from a surface event at 0°N, 0°E. For each station, the minimum delay time with respect to depth is displayed as a

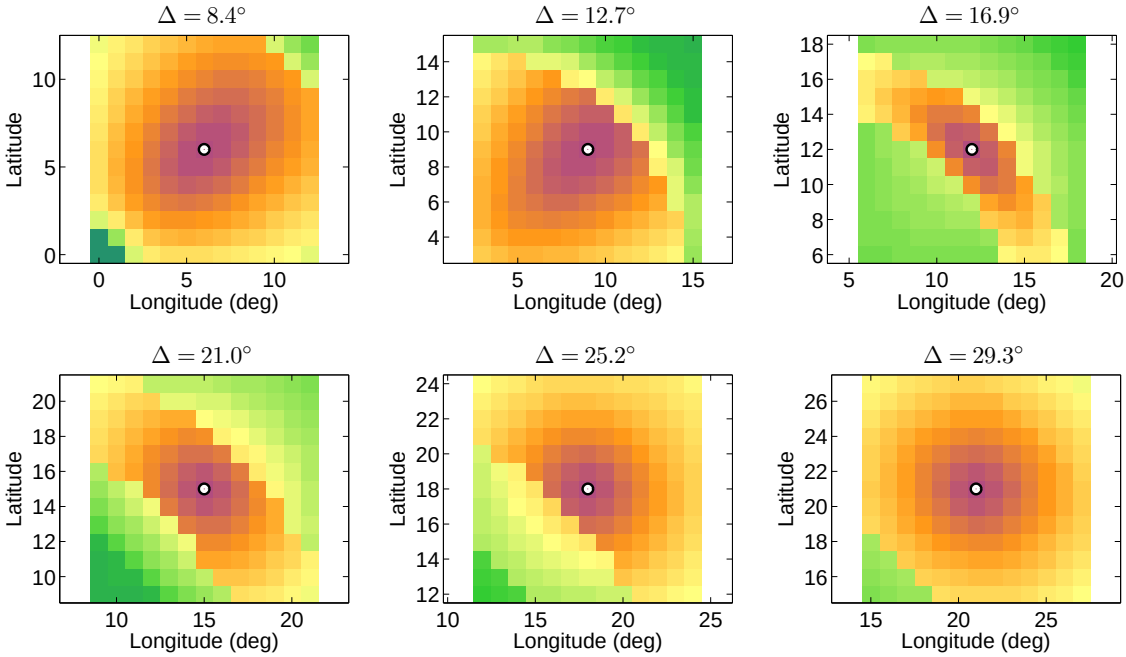

Figure 3: Correlation coefficient between the travel-time prediction error at a fixed reference station location (white dot) and at station locations surrounding the reference point. The assumed event location is at 0°N, 0°E (southwest of the stations). For each panel, the distance of the reference station from the event location is indicated as Δ, with Δ increasing from the top-left panel to the bottom-right panel. The color scale for correlation coefficient is the same as in Figure 2.

function of latitude and longitude. For a frequency of 1 Hz, the travel-time sensitivity peaks at a delay time of 0.25 s, so we may consider, as a rough rule of thumb, delay times of up to 0.5 s (yellow on the color scale) as defining the spatial extent of a travel-time sensitivity kernel. Under this criterion, we see that the lateral extent of the sensitivity kernels is roughly one-tenth the epicentral distance. For far-regional and teleseismic distances, this width becomes comparable to the horizontal correlation length of the velocity heterogeneity, at least as we have assumed it (300 km).

Figure 5 shows vertical sections through the delay time functions for various event-station distances. The left column spans regional distances from 11.5° to 15.5°. We see that up through an epicentral distance of $\Delta = 14.5°$ the 1 Hz travel time is sensitive to velocity structure from the Moho down to a depth that increases with distance, with the vertical extent of significant sensitivity ($\tau \leq 0.5$ s) eventually exceeding our assumed vertical correlation length of 60 km. Beyond 15°, the travel time begins to lose its sensitivity to the sub-Moho velocity and the sensitivity zone evolves into a more typical banana-doughnut shape localized around a geometrical ray (right column). Near cross-over distances, however, the sensitivity zone bifurcates (fourth panel down on right: $\Delta = 23.5°$). Although they lose their shallow sensitivity, the far-regional and teleseismic travel times still sense structure over a significant vertical extent.

CONCLUSIONS AND RECOMMENDATIONS

Our past efforts have developed numerical techniques for computing covariances between travel-time predictions along different event-station paths, using a model-based approach that combines stochastic descriptions of velocity anomalies in the Earth with the theoretical sensitivity of travel times to those anomalies. The techniques provide a useful tool for the theoretical investigation of how travel-time covariances behave for different stochastic Earth models and different raypath geometries.

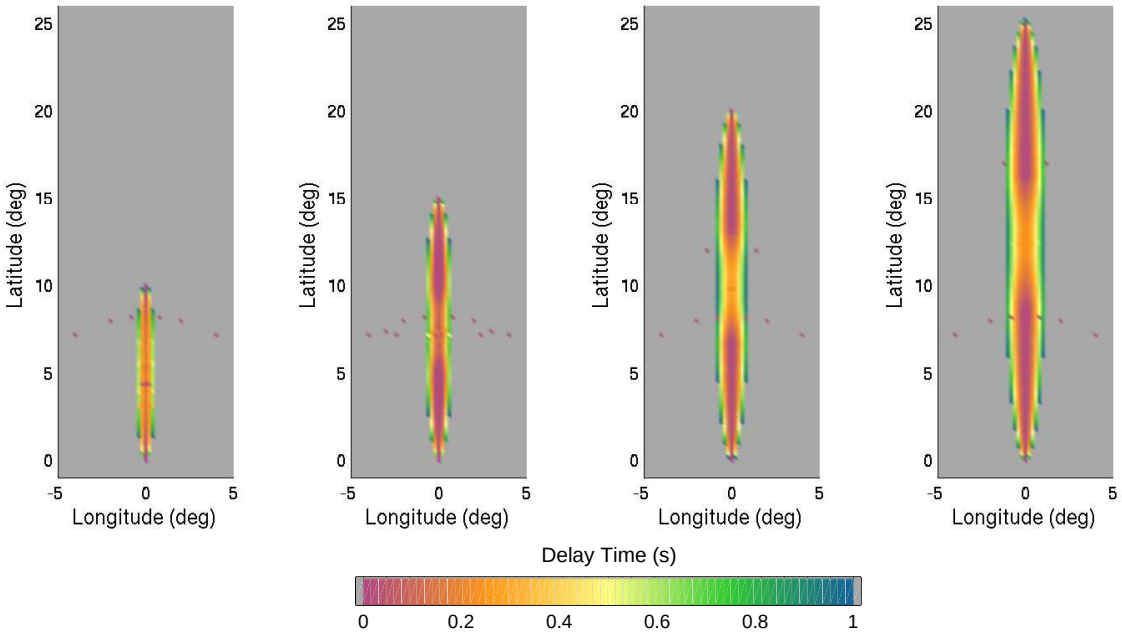

Figure 4: Delay time, minimized over depth, as a function of latitude and longitude for four source-receiver paths with epicentral distances of 10°, 15°, 20°, and 25° (left to right).

Applying the techniques with realistic assumptions about the statistical properties of velocity heterogeneity results in travel-time error vs. event-station distance plots that are in agreement with empirically developed curves (Figure 1). The often-noted decrease in travel-time error from regional to teleseismic distance is explained if the horizontal correlation length for velocity is greater than the vertical correlation length, and if the standard deviation of velocity decreases below the 410 km velocity discontinuity. Further, our calculations predict distinct breaks in residual correlation at the cross-overs between travel-time branches, the result of distinctly different ray paths for different branches. These breaks in travel-time correlation are exceedingly important for empirical travel-time calibration efforts and for proper estimation of the error covariance matrix that is used in seismic location.

We are currently investigating the effect of finite-frequency sensitivity kernels on travel-time covariances. Aside from the effect of velocity anomaly correlation, residuals along different paths will be correlated to the extent that their travel-time sensitivity kernels spatially overlap. Therefore, more spatially extensive sensitivity kernels are expected to result in greater residual correlation. In the preliminary work presented here we estimate the spatial extent of finite-frequency sensitivity kernels by computing delay times (relative to the geometric ray) for non-geometric paths. We find that the width of the sensitivity kernels for regional and teleseismic travel times, observed at a nominal frequency of 1 Hz, may be sufficiently large to affect travel-time correlations, especially for the far-regional Pn phase, whose sensitivity spans much of the upper mantle. This suggests that far-regional Pn residuals along similar event-station azimuths will be highly correlated, regardless of the correlation length of velocity heterogeneity.

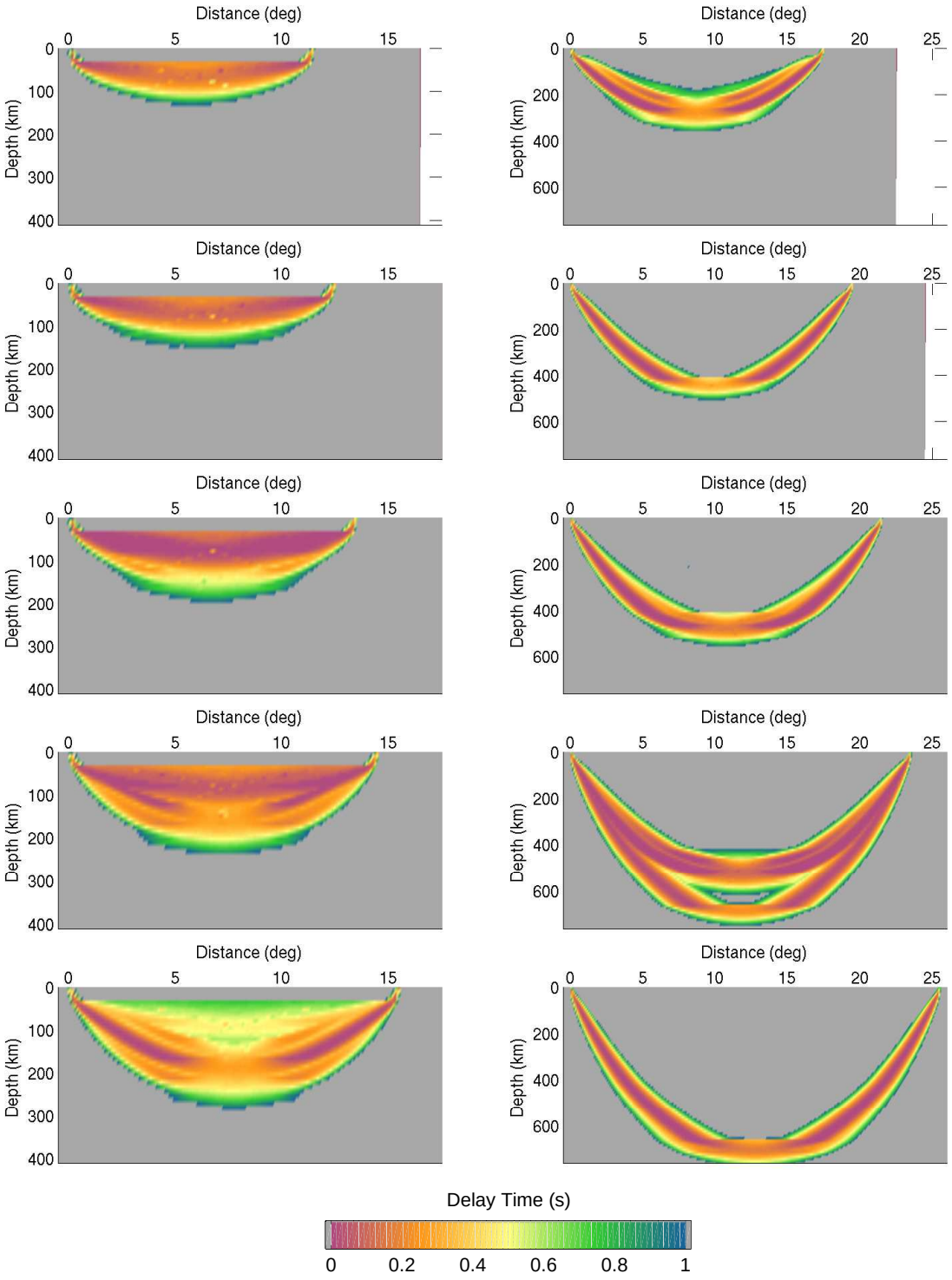

Figure 5: Vertical cross-section through the delay-time functions for ten event-station paths. In the left column, the epicentral distance varies from 11.5° to 15.5° with a 1° increment. In the right column, distance varies from 17.5° to 25.5° with a 2° increment.

REFERENCES

Bondar, I., S. Myers, E.R. Engdahl and E. Bergman (2004). Epicenter accuracy based on seismic network criteria, *Geophys. J. Int.* 156: 483–496.

Chang, A.C., R.H. Shumway, R.R. Blandford and B.W. Barker (1983). Two methods to improve location estimates—preliminary results, *Bull. Seism. Soc. Am.* 73: 281–295.

Dahlen, F.A., S.-H. Hung and G. Nolet (2000). Fréchet kernels for finite-frequency traveltimes I. Theory, *Geophys. J. Int.* 141: 157–174.

Flanagan, M.P., S.C. Myers and K.D. Koper (2007). Regional travel-time uncertainty and seismic location improvement using a three-dimensional a priori velocity model, *Bull. Seism. Soc. Am.* 97: 804–825.

Hung, S.-H., F.A. Dahlen and G. Nolet (2000). Fréchet kernels for finite-frequency traveltimes II. Examples, *Geophys. J. Int.* 141: 175–203.

Kennett, B.L.N., E.R. Engdahl and R. Buland (1995). Constraints on the velocity structure in the Earth from travel times, *Geophys. J. Int.* 122: 108–124.

Marquering, H., F.A. Dahlen and G. Nolet, 1999. Three-dimensional sensitivity kernels for finite-frequency traveltimes: the banana-doughnut paradox, *Geophys. J. Int.* 137: 805–815.

Rodi, W. and S.C. Myers (2007). Modeling travel-time correlations based on sensitivity kernels and correlated velocity anomalies, in *Proceedings of the 29th Monitoring Research Review: Ground-Based Nuclear Explosion Monitoring Technologies,* LA-UR-07-5613, Vol. 1, pp. 463–471.

Rodi, W., S.C. Myers and C.A. Schultz (2003). Grid-search location methods for ground-truth collection from local and regional seismic networks, in *Proceedings of the 25th Seismic Research Review—Nuclear Explosion Monitoring: Building the Knowledge Base,* LA-UR-03-6029, Vol. 1, pp. 311–319.

Ruppert, S., D. Dodge, A. Elliott, M. Ganzberger, T. Hauk and E. Matzel (2005). Enhancing seismic calibration research through software automation and scientific information management, in *Proceedings of the 27th Seismic Research Review: Ground-Based Nuclear Explosion Monitoring Technologies,* LA-UR-05-6407, Vol. 2.

Yang, X., I. Bondar, J. Bhattacharyya, M. Ritzwoller, N. Shapiro, M. Antolik, G. Ekstrom, H. Israelsson and K. McLaughlin (2004). Validation of regional and teleseismic travel-time models by relocating ground-truth events, *Bull. Seism. Soc. Am.* 94: 897–919.

Zhao, L., T.H. Jordan and C.H. Chapman (2000). Three-dimensional Fréchet differential kernels for seismic delay times, *Geophys. J. Int.* 141: 558–576.